Imaging small dielectric inclusions with polarization data

Patrick Bardsley, Maxence Cassier, Fernando Guevara Vasquez

Imaging small dielectric inclusions with polarization data

Patrick Bardsley[1], **Maxence Cassier**[2,*], **Fernando Guevara Vasquez**[3]

[1]Cirrus Logic, Salt Lake City, United States

[2]Aix Marseille Univ, CNRS, Centrale Marseille, Institut Fresnel, Marseille, France

[3]Mathematics Department, University of Utah, Salt Lake City, United States

[*]Email: maxence.cassier@fresnel.fr

Abstract

We present a method for imaging small dielectric inclusions in a homogeneous medium from polarization measurements. The problem is a generalization of phase-less imaging, with data being the coherency matrix of the electric field at an array of receivers. The data are obtained by illuminating the scatterers with a single point source with known position and polarization. The imaging consists of two steps. First we partially recover "the ideal data", i.e. when the full scattered field is measured on the array for three independent source polarizations. Second, we use an electromagnetic version of Kirchhoff imaging. We show that for high frequencies, the images we obtain are close to the ones obtained with ideal data. Resolution estimates of the reconstructed quantities and numerical results to illustrate our method are presented. A time domain interpretation of this imaging problem is left to the talk.

Keywords: Polarization imaging, Kirchhoff migration, phaseless imaging, coherency matrix.

1 Introduction and mathematical model

We consider the problem of imaging the position and polarizability tensor of N small dielectric polarizable inclusions in an homogeneous medium (with permeability μ) by using polarization data only. This is a common assumption in optics, where it is easier to measure polarization (a statistical property of light) than the full electrical field. We assume that the medium is probed by a single electric source whose position $\boldsymbol{x}_s \in \mathbb{R}^3$ is known and dipole moment is $\boldsymbol{j}_s'(\omega) \in \mathbb{C}^3$ at the frequency ω. Furthermore, the source and the two dimensional array $\mathcal{A}$ of receivers (within the plane $z = 0$) are supposed to be far from the inclusions. To model "white light" we assume its "rescaled dipole moment" $\boldsymbol{j}_s(\omega) = \mu\,\omega^2 \boldsymbol{j}_s'(\omega) \in \mathbb{C}^3$ is given at each frequency by a circular symmetric Gaussian random vector with zero mean $\langle \boldsymbol{j}_s(\omega) \rangle = 0$. The covariance of this vector is assumed known and determines the polarization state of the probing wave. It is given as $\boldsymbol{U}_s \boldsymbol{J}_s(\omega) \boldsymbol{U}_s^*$, where $\boldsymbol{J}_s(\omega)$ is a 2×2 complex positive definite matrix and $\boldsymbol{U}_s$ is 3×2 unitary matrix whose range $\mathrm{Ran}(\boldsymbol{U}_s)$ is the cross-range of the source. This corresponds to losing the range component of the source's polarization in the far field, where the probing wave is close to a plane wave near the inclusions [1].

At each realization, the source emits an incident wave: $\boldsymbol{E}_i(\boldsymbol{x};\omega) = \boldsymbol{G}(\boldsymbol{x}, \boldsymbol{x}_s;\omega)\, \boldsymbol{j}_s(\omega)$, where $\boldsymbol{G}(\boldsymbol{x}, \boldsymbol{x}_s;\omega)$ denotes the standard Dyadic Green tensor [4]. As the inclusions are assumed to be small with respect to the wavelength, they can be modelled as a point-like inclusion localized at $\boldsymbol{y}_n \in \mathbb{R}^3$ whose scattering properties are determined by a polarizability tensor $\boldsymbol{\alpha}'(\boldsymbol{y}_n;\omega)$ for $n = 1, \dots, N$ that is a 3×3 complex symmetric matrix. We denote by $\boldsymbol{\alpha}(\boldsymbol{y}_n) = \mu\,\omega^2 \boldsymbol{\alpha}'(\boldsymbol{y}_n;\omega)$ "the rescaled polarizability tensor", assumed here to be frequency independent. The incident wave is then reflected and the resulting scattered field (see [4]) is given under the first Born approximation by: $\boldsymbol{E}_{\mathrm{s}}(\boldsymbol{x};\omega) = \boldsymbol{\Pi}(\boldsymbol{x};\omega)\boldsymbol{j}_s(\omega)$ with

$$\boldsymbol{\Pi}(\boldsymbol{x};\omega) = \sum_{n=1}^{N} \boldsymbol{G}(\boldsymbol{x}, \boldsymbol{y}_n;\omega)\, \boldsymbol{\alpha}(\boldsymbol{y}_n)\, \boldsymbol{G}(\boldsymbol{y}_n, \boldsymbol{x}_s;\omega).$$

Finally, one records at each receiver $\boldsymbol{x}_r \in \mathcal{A}$ the 2×2 coherency matrix:

$$\psi(\boldsymbol{x}_r;\omega) = \left\langle \left[(\, \boldsymbol{E}(\boldsymbol{x}_r;\omega) \boldsymbol{E}(\boldsymbol{x}_r;\omega)^\top \right]_{1:2,1:2} \right\rangle, \quad (1)$$

that encodes the polarization of the total field $\boldsymbol{E} = \boldsymbol{E}_i + \boldsymbol{E}_s$ on $\mathcal{A}$ (where $\langle\cdot\rangle$ is the expectation).

2 Kirchhoff imaging with ideal data

We consider now the case of ideal data, that is when one can measure $\boldsymbol{\Pi}(\boldsymbol{x};\omega)$ for $\boldsymbol{x} \in \mathcal{A}$ or equivalently the scattered field for three independent source's dipole moments. We use a matrix-valued electromagnetic version of the Kirchhoff imaging function [3]:

$$\mathcal{I}[\boldsymbol{\Pi}](\boldsymbol{y};\omega) = \int_{\mathcal{A}} d\boldsymbol{x}_r \overline{\boldsymbol{G}(\boldsymbol{x}_r, \boldsymbol{y};\omega)} \boldsymbol{\Pi}(\boldsymbol{x}_r;\omega) \overline{\boldsymbol{G}(\boldsymbol{x}_s, \boldsymbol{y};\omega)}.$$

We denote by $\boldsymbol{U}_r = [\boldsymbol{e}_1, \boldsymbol{e}_2]$ (where $(\boldsymbol{e}_1, \boldsymbol{e}_2, \boldsymbol{e}_3)$ is the canonical basis of $\mathbb{R}^3$) the 3×2 unitary matrix whose range is the cross-range of $\mathcal{A}$. We extract from $\mathcal{I}$ a stable reconstruction [1, 3] of the position $\boldsymbol{y}_n$ and of the 2×2 block $\widetilde{\boldsymbol{\alpha}}_n = \boldsymbol{U}_r^* \boldsymbol{\alpha}(\boldsymbol{y}_n)\boldsymbol{U}_s$ of the polarizability tensor $\boldsymbol{\alpha}(\boldsymbol{y}_n)$ (up to a complex phase). The other components of $\boldsymbol{\alpha}(\boldsymbol{y}_n)$ are lost in this regime of propagation. In the Fraunhofer regime [1], resolution estimates for the reconstruction of these two quantities are given (as in acoustics) by the Rayleigh criterion in cross-range and by c/B in range (where the constant c is the wave propagation speed and B the frequency bandwidth of the data $\boldsymbol{\Pi}(\cdot, \omega)$). Moreover, one shows that

$$\mathcal{I}[\boldsymbol{\Pi}](\boldsymbol{y}; \omega) \approx \mathcal{I}[\boldsymbol{U}_r \widetilde{\boldsymbol{\Pi}} \boldsymbol{U}_s^*](\boldsymbol{y}; \omega) \text{ with } \widetilde{\boldsymbol{\Pi}} = \boldsymbol{U}_r^* \boldsymbol{\Pi} \boldsymbol{U}_s.$$

Thus, instead of using $\boldsymbol{\Pi}$, one can image as well with $\boldsymbol{U}_r \widetilde{\boldsymbol{\Pi}} \boldsymbol{U}_s^*$, i.e. the ideal data $\boldsymbol{\Pi}$ projected on the left on the cross-range of the array and on the right on the cross-range of the source.

3 The Phase-less imaging method

The strategy we use for imaging generalizes the approach for scalar waves of [2]. One first preprocesses the data $\boldsymbol{\psi}(\boldsymbol{x}_r; \omega)$ to calculate the matrix $p(\boldsymbol{\psi}) = \boldsymbol{U}_r \widetilde{\boldsymbol{\Pi}} \boldsymbol{U}_s^* + \text{error terms}$. It consists in particular to partially recover the data $\boldsymbol{U}_r \widetilde{\boldsymbol{\Pi}} \boldsymbol{U}_s^*$ by eliminating the contribution of the incident field $\boldsymbol{E}_i$ in (1). The remaining error terms are antilinear and sesquilinear in $\widetilde{\boldsymbol{\Pi}}$. The key is that these terms do not affect the Kirchhoff images for high frequencies. Indeed, one shows [1] via a stationary phase argument and under mild assumptions on the geometry of the problem that the imaging functions with either $p(\boldsymbol{\psi})$ or $\boldsymbol{\Pi}$ data are similar, i.e. as $\omega \to \infty$ we have

$$\mathcal{I}[p(\boldsymbol{\psi})](\boldsymbol{y}; \omega) = \mathcal{I}[\boldsymbol{U}_r \widetilde{\boldsymbol{\Pi}} \boldsymbol{U}_s^*](\boldsymbol{y}; \omega) + o(1).$$

Our method is illustrated in figure 1 where the medium contains two dipoles located at $\boldsymbol{y}_1 = (-6, 4, 105)\lambda_0$ and $\boldsymbol{y}_2 = (7, 4, 105)\lambda_0$ with λ_0 the central wavelength of B. To image the position, we use the Frobenius norm $\|\widetilde{\boldsymbol{\alpha}}(\cdot)\|_F$ of the recovered polarizability tensor. To visualize the polarization tensor (up to a complex phase) we visualize $\operatorname{Re}\widetilde{\boldsymbol{\alpha}} = 1/2(\widetilde{\boldsymbol{\alpha}} + \overline{\widetilde{\boldsymbol{\alpha}}})$ and $\operatorname{Im}\widetilde{\boldsymbol{\alpha}} = (1/2i)(\widetilde{\boldsymbol{\alpha}} - \overline{\widetilde{\boldsymbol{\alpha}}})$, which are real non-symmetric matrices. We visualize 2×2 real matrices $\boldsymbol{A}$ with the ellipse $\mathcal{E}(\boldsymbol{A}) = \{\boldsymbol{A}\boldsymbol{v} \mid \|\boldsymbol{v}\|_2 = 1\}$. To emphasize that the matrices are not symmetric, we also display the vectors $\sigma_1 \boldsymbol{v}_1$ and $\sigma_2 \boldsymbol{v}_2$ as axes, where the σ_j are the singular values and $\boldsymbol{v}_j$ the right singular vectors of $\boldsymbol{A}$.

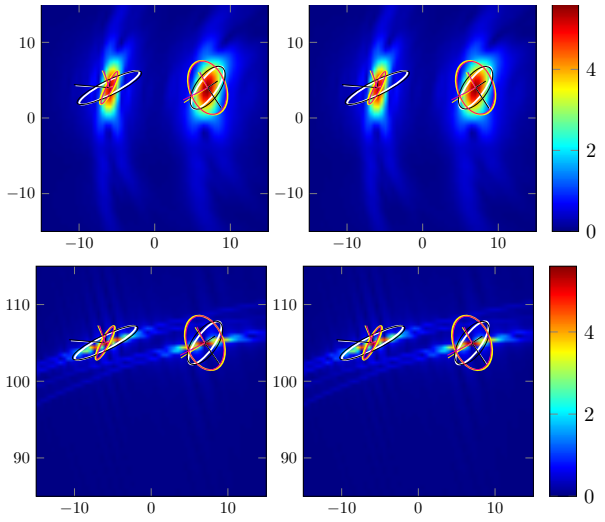

Figure 1: Cross-range (top) and range (bottom) images of $\|\widetilde{\boldsymbol{\alpha}}(\cdot)\|_F$. The columns show reconstructions with $\boldsymbol{\Pi}$ (left) and with $p(\boldsymbol{\psi})$ (right). Here (up to a reference phase [1]) the true tensor $\operatorname{Re}\widetilde{\boldsymbol{\alpha}}$ (resp. $\operatorname{Im}\widetilde{\boldsymbol{\alpha}}$) is depicted by the white (resp. yellow) ellipses/axes, whereas the recovered tensor is depicted using black (real part) and magenta (imaginary part) ellipses/axes.

This work was partially supported by the National Science Foundation grant DMS-1411577. The work of M. C. was supported by Simons Foundation grant #376319 (M. I. Weinstein).

References

[1] P. Bardsley, M. Cassier and F. Guevara Vasquez, Imaging small polarizable scatterers with polarization data, *Inverse Problems* **34** (10) (2018), pp. 104002.

[2] P. Bardsley and F. Guevara Vasquez, Kirchhoff migration without phases, *Inverse Problems* **32** (10) (2016), pp. 105006.

[3] M. Cassier and F. Guevara Vasquez, Imaging polarizable dipoles, *SIAM J. Imaging Sci.* **10** (3) (2017), pp. 1381–1415.

[4] L. Novotny and B. Hecht, *Principles of nano-optics*, Cambridge univ. press, 2012.